

Deep Cox Mixtures for Survival Regression

Chirag Nagpal^{1,2}, Steve Yadlowsky¹, Negar Rostamzadeh¹ and Katherine Heller¹

¹Google Brain

²Carnegie Mellon University

ABSTRACT

Survival analysis is a challenging variation of regression modeling because of the presence of censoring, where the outcome measurement is only partially known, due to, for example, loss to follow up. Such problems come up frequently in medical applications, making survival analysis a key endeavor in biostatistics and machine learning for healthcare, with Cox regression models being amongst the most commonly employed models. We describe a new approach for survival analysis regression models, based on learning mixtures of Cox regressions to model individual survival distributions. We propose an approximation to the Expectation Maximization algorithm for this model that does hard assignments to mixture groups to make optimization efficient. In each group assignment, we fit the hazard ratios within each group using deep neural networks, and the baseline hazard for each mixture component non-parametrically.

We perform experiments on multiple real world datasets, and look at the mortality rates of patients across ethnicity and gender. We emphasize the importance of calibration in healthcare settings and demonstrate that our approach outperforms classical and modern survival analysis baselines, both in terms of discriminative performance and calibration, with large gains in performance on the minority demographics.

KEYWORDS

survival analysis, time-to-event, censored data, calibration

ACM Reference Format:

Chirag Nagpal^{1,2}, Steve Yadlowsky¹, Negar Rostamzadeh¹ and Katherine Heller¹. 2021. Deep Cox Mixtures for Survival Regression. In *Conference '21*. ACM, New York, NY, USA, 22 pages. <https://doi.org/10.1145/nnnnnnn.nnnnnnn>

1 INTRODUCTION

The importance of survival analysis models in medical applications cannot be overstated. These models support physicians and epidemiologists in clinical decision making based on data-driven evidence about patients' likelihood of survival characteristics based on biological measurements and demographic information about the patients. In this paper, we focus on estimating the patient's risk of an event T of interest, specifically the conditional survival

curve, $\mathbb{P}(T > t|X)$. Typically events include death, or the presence or progression of a health condition.

The one frequent challenge with estimating the survival curve is that outcomes are typically censored, meaning that the outcome is unknown for some patients due to lack of follow up or independent competing events. Luckily, censoring is relatively straightforward to deal with in certain commonly used survival analysis models that make the proportional hazards assumption, such as the Cox regression model, or Faraggi-Simon deep neural network model. Unfortunately, in many important cases, the proportional hazards assumption does not hold, leading to poor calibration of patients' estimated survival curve, even if the model can rank patients well.

In fact, many recent deep learning approaches demonstrate significant improvement in ranking patients' survival according to discriminative measures such as the concordance index (C -index). However, the C -index measures pairwise ranking ability and disregards the absolute value of the actual estimated risk score akin to metrics of evaluating binary classification like the Receiver Operating Characteristic.

We generalize the proportional hazards assumption via a mixture model, by assuming that there are latent groups and within each, the proportional hazards assumption holds. We develop an approximate Expectation-Maximization (EM) learning algorithm to estimate the latent groups and parameters of conditional survival curves within each group. Due to the non-collapsibility of the hazard ratio, the model after integrating out over these latent groups is not restricted by the strong assumption of proportional hazards and by allowing the model to flexibly choose these latent groups, we can build a more expressive survival analysis model. To make the learning algorithm tractable, we approximate the Maximization step (M-step) by hard assignment of each patient to a latent group, and approximate the baseline survival curves in the Expectation step (E-step) with a spline estimate. Our approach allows the hazard ratio in each latent group to be flexibly modeled by a deep neural network, allowing us to take advantage of many of the recent improvements in neural network modeling of patient data.

In our experiments, we show that the added flexibility of this mixture of proportional hazards models allows us to improve the calibration of the estimated conditional survival curves, while maintaining excellent discriminative performance; that is, without requiring a performance trade-off. We find that the largest improvements to calibration occur among minority groups, and emphasize the need for evaluating performance on such groups, which can often go unnoticed on dataset-wide performance statistics. Our model is implemented in tensorflow and source code of our experiments is open source and publicly available at https://github.com/chiragnagpal/deep_cox_mixtures.

Address correspondence to: Chirag Nagpal, <chiragn@cs.cmu.edu>

Permission to make digital or hard copies of all or part of this work for personal or classroom use is granted without fee provided that copies are not made or distributed for profit or commercial advantage and that copies bear this notice and the full citation on the first page. Copyrights for components of this work owned by others than ACM must be honored. Abstracting with credit is permitted. To copy otherwise, or republish, to post on servers or to redistribute to lists, requires prior specific permission and/or a fee. Request permissions from permissions@acm.org.

Conference '21, ,

© 2021 Association for Computing Machinery.

ACM ISBN 978-x-xxxx-xxxx-x/YY/MM... \$15.00

<https://doi.org/10.1145/nnnnnnn.nnnnnnn>

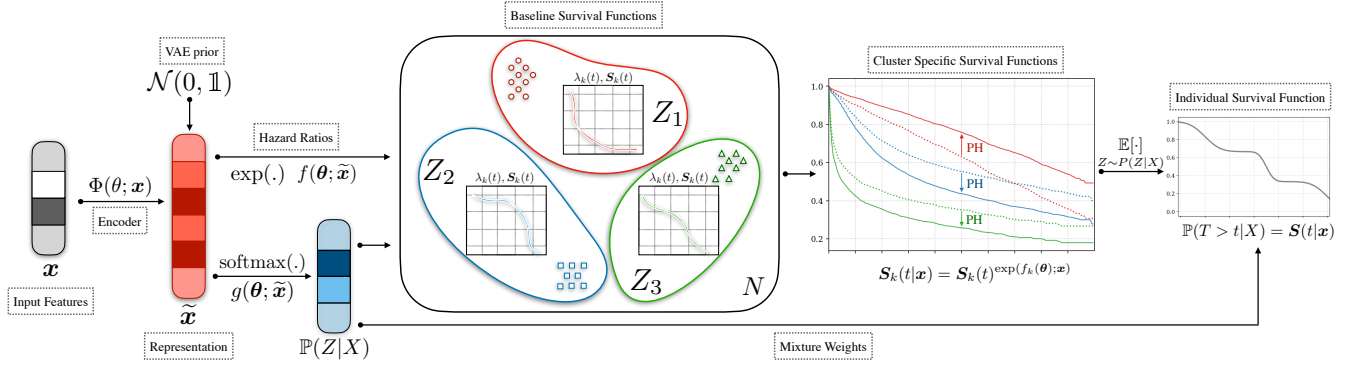


Figure 1: Deep Cox Mixtures: Representation of the individual covariates x are generated using an encoding neural network. The output representation \tilde{x} then interacts with linear functions f and g that determine the proportional hazards within each cluster $Z \in \{1, 2, \dots, K\}$ and the mixing weights $\mathbb{P}(Z|X)$ respectively. For each cluster, baseline survival rates $S_k(t)$ are estimated non-parametrically. The final individual survival curve $S(t|x)$ is an average over the cluster specific individual survival curves weighted by the mixing probabilities $\mathbb{P}(Z|X = x)$.

2 THE DEEP COX MIXTURE MODEL

2.1 Notation

We consider a dataset of right censored observations $\mathcal{D} = \{(x_i, \delta_i, u_i)\}_{i=1}^N$ of three tuples, where x_i are the covariates of an individual i , δ_i is an indicator of whether an event occurred or not and u_i is either the time of event or censoring as indicated by δ_i .

We consider a maximum likelihood (MLE) based approach to learning $S(t|x) = \mathbb{P}(T > t|X = x)$ from the data. Recall that the survival distribution $S(t|x)$ is isomorphic to the cumulative hazard function $\Lambda(t|x)$, and under continuity, this is equivalent to the hazard function $\lambda(t|x)$. As a result, we will refer them in the parameters of the likelihood interchangeably. Lin (2007) shows that the likelihood of the observed data \mathcal{D} is, up to constant factors,

$$\mathcal{L}(\Lambda) = \prod_{i=1}^{|\mathcal{D}|} (\lambda(u_i|x_i))^{\delta_i} S(u_i|x_i). \quad (1)$$

In the following sections, we show how plugging in specific functional forms for $S(t|x)$ allows us to derive survival function estimators.

2.2 MLE for the standard Cox PH model

The key idea behind the Cox model is to assume that the conditional hazard of an individual, is $\lambda(t|x) = \lambda_0(t) \exp(f(\theta, x))$, where f is typically a linear function. Under the Cox model, the full likelihood as in equation 1 is

$$\mathcal{L}(\theta, \Lambda_0) = \prod_{i=1}^{|\mathcal{D}|} \left(\lambda_0(u_i) \exp(f(\theta, x_i)) \right)^{\delta_i} S_0(u_i) \exp(f(\theta, x_i)) \quad (2)$$

Cox and the discussion of his paper by Breslow, suggest deriving a maximum likelihood estimate of θ by maximizing the partial likelihood, $\mathcal{P}\mathcal{L}(\theta)$ defined below, and using the following estimator

of the baseline survival function $\Lambda_0(\cdot)$,

$$\mathcal{P}\mathcal{L}(\theta) = \prod_{i:\delta_i=1} \frac{\exp(f(\theta; x_i))}{\sum_{j \in \mathcal{R}(t_i)} \exp(f(\theta; x_j))}, \quad (3)$$

$$\hat{\Lambda}_0(t) = \sum_{i:t_i < t} \frac{1}{\sum_{j \in \mathcal{R}(t_i)} \exp(f(\hat{\theta}; x_j))}, \quad (4)$$

where $\mathcal{R}(t_i)$ is the ‘risk set’ – the set of individuals that survived beyond time t_i .

2.3 Proposed Model

In the case of DCM we propose an extension to the Cox model, modeling an individual’s survival function using a finite mixture of K Cox models, with the assignment of an individual i to each latent group mediated by a gating function $g(\cdot)$. The full likelihood for this model is

$$\mathcal{L}(\theta, \Lambda_k) = \prod_{i=1}^{|\mathcal{D}|} \int_Z (\lambda(u_i|x_i))^{\delta_i} S_k(u_i|x_i) \mathbb{P}(Z = k|x_i).$$

where, $\lambda(u_i|x_i) = \lambda_k(u_i) \exp(f_k(\theta, x_i))$

$$S_k(u_i|x_i) = S_k(u_i) \exp(f_k(\theta, x_i))$$

$$\mathbb{P}(Z = k|X = x_i) = \text{softmax}(g(\theta; x_i)) \quad (5)$$

Architecture: We allow the model to learn representations for the covariates x_i by passing them through an encoding neural network, $\Phi(\cdot)$. This representation then interacts with linear functions f and g defined on $\mathbb{R}^h \rightarrow \mathbb{R}^k$; that determine the log hazard ratios and the mixture weights respectively. The set of parameters for the encoder Φ and the linear functions f and g are jointly notated as θ . We experiment with a simple feed forward MLP and a variational auto-encoder for $\Phi(\cdot)$. The parameters of the MLP and the VAE are learnt jointly during learning. For the VAE variant the encoder and the decoder architecture is kept the same. We also experiment with a variant that doesn’t use representation learning and thus the functions f and g are linear and restricted to operate on the

original features \mathbf{x} . Figure 1 provides a schematic description of our approach.

2.4 Learning

Notice that under the model in Eq. 5, the corresponding partial likelihood is not independent of $\lambda(\cdot)$, the hazard rate. We hence cannot directly optimize the partial likelihood to perform parameter learning. This inference complexity is outlined in Appendix A.1.

Since our model requires inference over the latent assignments Z for learning the Expectation Maximization (Dempster et al., 1977) algorithm is a natural approach to perform inference. The major challenge to applying exact EM lies in the fact that under the our model requires a summation over all possible combinations of latent assignments and which is intractable to compute. We propose an approximate, Monte Carlo EM (Wei and Tanner, 1990; Song et al., 2016) algorithm involving the drawing of posterior samples to learn the parameters, θ and the baseline survival functions $\{S_k(\cdot)\}_{i=1}^K$.

E-Step: Involves estimating the posteriors of Z , $\gamma_i \propto \mathbb{P}(T = t|X, Z)^{\delta_i} \mathbb{P}(T > t|X, Z)^{1-\delta_i}$. The Breslow estimator only gives us the estimates of the survival rates, thus computing the posterior counts, $h_i \propto \mathbb{P}(T = t_i|Z, X)$ for the uncensored instances challenging. We mitigate this by interpolating the Baseline Survival Rate for each latent group, $S_k(\cdot)$ using a polynomial spline. Equation 6 provides the interpolated event probability estimates. (Appendix A.2 describes this in detail.)

$$\begin{aligned} \widehat{\mathbb{P}}(T > t|X = \mathbf{x}_i, Z = k) &= \widetilde{S}_k(t)^{\exp(f_k(\theta; \mathbf{x}_i))} \text{ and,} \\ \widehat{\mathbb{P}}(T = t|X = \mathbf{x}_i, Z = k) &= \\ &= \exp(f_k(\theta; \mathbf{x}_i)) \frac{\widehat{\mathbb{P}}(T > t|\mathbf{x}_i, Z = k)}{\widetilde{S}_k(t)} \frac{\partial \widetilde{S}_k(t)}{\partial t} \end{aligned} \quad (6)$$

Here, $\widetilde{S}_k(t)$ is the baseline survival rate interpolated with a polynomial spline.

M-Step: Once the posterior counts γ_i are obtained, the M-Step involves learning maximizing the corresponding $Q(\cdot)$ function given as

$$Q(\theta) = \sum_{i=1}^{|\mathcal{D}|} \sum_k \gamma_i^k \ln \mathbb{P}(Z|X) + \gamma_i^k \ln \mathbb{P}(t|Z, X); \quad (7)$$

where, $\gamma_i \propto \mathbb{P}(T|X, Z)$

Notice that the γ_i^k are soft counts ($\gamma_i \in [0, 1]$) making parameter inference for the term $\mathbb{P}(T|Z, X)$ intractable. Motivated from Monte-Carlo EM methods We instead sample hard posterior counts $\zeta_i \sim \text{Categorical}(\gamma_i)$.

We replace this with hard posterior counts for the second term, $\ln \mathbb{P}(t|Z, X)$

$$\begin{aligned} \overline{Q}(\theta) &= \sum_{i=1}^{|\mathcal{D}|} \sum_k \gamma_i^k \ln \mathbb{P}(Z|X) + \zeta_i^k \ln \mathbb{P}(t|Z, X); \\ &\text{where, } \zeta_i \sim \text{Categorical}(\gamma_i) \end{aligned} \quad (8)$$

Note that $\mathbb{E}[\overline{Q}(\cdot)] = Q(\cdot)$. Thus, $\overline{Q}(\cdot)$ is an unbiased estimate of the exact $Q(\cdot)$

The first term in $\overline{Q}(\cdot)$ can be optimized using gradient based approaches. The second term can be re-written as a sum over k latent groups variables.

$$\begin{aligned} \overline{Q}(\theta) &= \sum_{i=1}^{|\mathcal{D}|} \sum_k \gamma_i^k \ln \mathbb{P}(Z|X) + \mathbb{1}\{\zeta_i = k\} \ln \mathbb{P}(t|Z, X) \\ &= \sum_{i=1}^{|\mathcal{D}|} \sum_k \gamma_i^k \ln \mathbb{P}(Z|X) + \sum_{i=1}^{|\mathcal{D}|} \sum_k \mathbb{1}\{\zeta_i = k\} \ln \mathbb{P}(t|Z, X) \\ &= \sum_{i=1}^{|\mathcal{D}|} \sum_k \gamma_i^k \ln \mathbb{P}(Z|X) + \sum_k \sum_{i=1}^{|\mathcal{D}_k|} \ln \mathbb{P}(t|Z, X) \end{aligned} \quad (9)$$

(Here, \mathcal{D}_k is the set of all \mathcal{D} with $\zeta_i = k$)

Now using the fact that the Proportional Hazards assumption holds within each group \mathcal{D}_k we arrive at the form of the $Q(\cdot)$ that we optimize in each minibatch as

$$\widehat{Q}(\theta) = \sum_{i \in \mathcal{D}_b} \sum_k \gamma_i^k \ln \text{softmax}(g(\theta; \mathbf{x}_i)) + \sum_k \ln \mathcal{P} \mathcal{L}(\mathcal{D}_b^k; \theta)$$

Here, \mathcal{D}_b^k is the subset of all individuals that have $\zeta_i = k$ within the minibatch b and $\mathcal{P} \mathcal{L}(\cdot)$ is the partial likelihood as defined in Equation 3. Thus, the use of hard counts ζ effectively reduces the problem to learning K separate Cox models allowing us to maximize the partial likelihood independently within each $k \in K$.

The parameters of the encoder are also updated during the **M-Step** by adding the loss corresponding to the VAE. Altogether the loss function for optimization is

$$\text{Loss}(\theta; \mathcal{D}_b) = \widehat{Q}(\theta; \mathcal{D}_b) + \alpha \cdot \text{VAE-Loss}(\theta; \mathcal{D}_b) \quad (10)$$

Here, the VAE-Loss is the Evidence Lower Bound for the VAE with representations drawn from a zero mean and identity covariance gaussian prior as in Kingma and Welling (2013).

Algorithm ?? describes the learning procedure for DCM. We sample minibatches \mathcal{D}_b from the data \mathcal{D} and compute the soft and hard posterior counts, $\{\gamma_i, \zeta_i\}_{i \in \mathcal{D}_b}$ for each batch. This is followed by the **M-Step** involving a gradient update the parameter set θ . Finally, we update the Baseline Survival Splines, \widetilde{S}_k computed using the Breslow's estimator for each cluster. Note that the Breslow's estimator is computed over the full batch, \mathcal{D} . This does not involve gradient computation and so is not expensive.

2.5 Inference

Following Equation 5, at test time the estimated risk of an individual at time t is given as

$$\begin{aligned} \widehat{\mathbb{P}}(T > t|X = \mathbf{x}_i) &= \mathbb{E}_{Z \sim \widehat{\mathbb{P}}(Z|X)} [\widehat{\mathbb{P}}(T|X = \mathbf{x}_i, Z)] \\ &= \sum_k \widetilde{S}_k(t)^{\exp(f(\theta; \mathbf{x}_i))} \times \text{softmax}_k(g(\theta; \mathbf{x}_i)) \end{aligned} \quad (11)$$

In this section we describe the datasets, the survival analysis tasks and baselines we compare DCM against. We also describe the corresponding metrics we employ for evaluation.

Algorithm 1: Learning for DCM

Input : Training set, $\mathcal{D} = \{(x_i, t_i, \delta_i)_{i=1}^N\}$; batches, B ;
while <not converged> **do**
 for $b \in \{1, 2, \dots, B\}$ **do**
 $\mathcal{D}_b \leftarrow \text{sampleMiniBatch}(\mathcal{D})$
 $\{\gamma_i\}_{i=1}^B \leftarrow \text{E-Step}(\theta, \{\tilde{S}_k\}_{i=1}^K)$;
 $\{\zeta_i\}_{i=1}^B \sim \text{Categorical}(\gamma)$;
 $\theta \leftarrow \text{M-Step}(\theta, \{\zeta_i, \gamma_i\}_{i=1}^B)$;
 for $k \in \{1, 2, \dots, K\}$ **do**
 $\hat{S}_k \leftarrow \text{breslow}(\theta, \{(t_i, \delta_i)\}_{i=1; \zeta_i=k}^{|\mathcal{D}|})$;
 $\tilde{S}_k \leftarrow \text{splineInterpolate}(\hat{S}_k)$;
 end
 end
end
Return : learnt parameters, θ ;
 baseline survival splines $\{\tilde{S}_k\}_{i=1}^K$

2.6 Datasets

We experiment with the following real world, publicly available survival analysis datasets:

FLCHAIN (Assay of Serum Free Light Chain): This is a public dataset introduced by [Dispenzieri et al. \(2012\)](#) aiming to study the relationship between serum free light chain and mortality. It includes covariates like age, gender, serum creatinine and presence of monoclonal gammopathy. We removed all the individuals with missing covariates and experiment with the remaining subset of 6,524 individuals. Out of this subset 45% of the participants were coded as female and are considered as ‘minority’ in our experiments.

SUPPORT (Study to understand prognoses and preferences for outcomes and risks of treatments ([Connors et al., 1995](#)): Dataset from study instituted to understand patient survival for 9,105 terminally ill patients on life support. The median survival time for the patients in the study was 58 days. Out of the 9,105 patients a majority 79% were coded as ‘White’, while the rest were coded as ‘Black’, ‘Hispanic’ and ‘Asian’.

SEER (Surveillance, Epidemiology and End Results Study)^{*}: This dataset consists of survival characteristics of oncology patients taken from cancer registries covering about one-third of the US Population. For our study we consider a cohort of patients over a 15 year period from 1992-2007 diagnosed with breast cancer with a median survival time of 55 months. A majority (76%) of the patients were coded as ‘White’ and the rest were other minorities consisting of ‘Blacks’, ‘American Indians’, ‘Asians’, etc.[†]

Our choice of datasets encompass varying ranges of dimensionality of covariates, levels of censoring and size vis-a-vis the minority demographics. Table 1 describes some summary statistics of the considered datasets. Figure 2 compares the baseline survival rates for the majority and minorities in the SEER and SUPPORT dataset.

^{*}<https://seer.cancer.gov/>

[†]SEER has a very intricate coding pattern vis-a-vis race. Refer to https://seer.cancer.gov/tools/codingmanuals/race_code_pages.pdf for details.

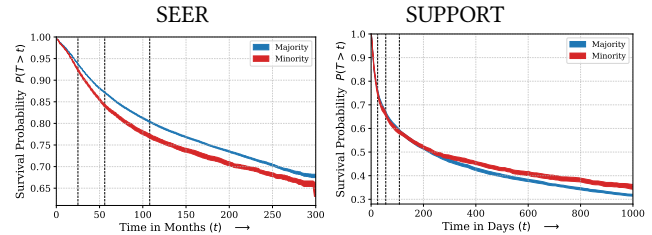


Figure 2: Base survival rates for the majority (White) vs. the other demographics in the SEER dataset estimated with a Kaplan-Meier estimator. Notice that the baseline survival rates differ across groups. Dashed lines represent the 25th, 50th and 75th quantiles of event times.

Notice that base survival rates across demographics can vary considerably over time.

2.7 Baselines

We compare the proposed DCM against the following baselines.

Accelerated Failure Time (AFT): This is an extension of generalized linear models to the survival setting with censored data. The target variable is assumed to follow a Weibull distribution and the shape and scale parameters are modelled as linear functions of the covariates. Parameter learning is performed using Maximum Likelihood Estimation.

Deep Survival Machines (DSM) ([Nagpal et al., 2020](#)): This is another fully parametric approach and improves on the Accelerated Failure Time model by modelling the event time distribution as a fixed size mixture over Weibull or Log-Normal distributions. The individual mixture distributions are themselves parametrized with neural networks allowing to learn complex non-linear representations of the data.

Deep Hit (DHT) ([Lee et al., 2018](#)): A discrete time model, DeepHit is a popular Neural Network approach that involves discretizing the event outcome space and treating the survival analysis problem as a multiclass classification problem over the discrete intervals.

Cox Proportional Hazards (CPH): CPH assumes that individuals across the population have constant proportional hazards overtime.

Faraggi-Simon Net (FSN)/DeepSurv ([Faraggi and Simon, 1995](#); [Katzman et al., 2018](#)): An extension to the CPH model, FSN involves modelling the proportional hazard ratios over the individuals with Deep Neural Networks allowing the ability to learn non linear hazard ratios.

Random Survival Forest (RSF) ([Ishwaran et al., 2008](#)): RSF is an extension of Random Forests to the survival settings where risk scores are computed by creating Nelson-Aalen estimators in the splits induced by the Random Forest.

Table 1: Summary statistics for the datasets used in the experiments.

Dataset	N	d	Censoring (%)	Minority Class (%)	Event Quantiles		
					t = 25th	t = 50th	t = 75th
SUPPORT	9,105	44	31.89%	Non-White (21.02%)	14	58	252
FLCHAIN	6,524	8	69.93%	Female (44.94%)	903.25	2085	3246
SEER	55,993	168	72.82%	Non-White (23.77%)	25	55	108

The full set of hyper parameter we perform grid search on is deferred to Appendix C.

2.8 Evaluation Metrics

We compare the performance of DCM against baselines in terms of both discriminative performance and calibration using the following metrics:

Area under ROC Curve (AUC): Involves treating the survival analysis problem as binary classification at different quantiles of event times and computing the corresponding area under the ROC curve.

Time Dependent Concordance Index (C^{td}): Concordance Index estimates ranking ability by exhaustively comparing relative risks across all pairs of individuals in the test set. We employ the ‘Time Dependent’ variant of Concordance Index that truncates the pairwise comparisons to the events occurring within a fixed time horizon.

$$C^{td}(t) = \mathbb{P}(\hat{F}(t|\mathbf{x}_i) > \hat{F}(t|\mathbf{x}_j) | \delta_i = 1, T_i < T_j, T_i \leq t)$$

Expected ℓ_1 Calibration Error (ECE): The ECE measures the average absolute difference between the observed and expected (according to the risk score) event rates, conditional on the estimated risk score. At time t , let the predicted risk score be $R(t) = \widehat{\mathbb{P}}(T > t|X)$. Then, the ECE approximates

$$ECE(t) = \mathbb{E} \left[\left| \mathbb{P}(T > t|R(t)) - R(t) \right| \right]$$

by partitioning the risk scores R into q quantiles $\{[r_j, r_{j+1})\}_{j=1}^q$.

Brier Score (BS): The Brier Score involves computing the Mean Squared Error around the binary forecast of survival at a certain event quantile of interest. Brier Score is a proper scoring rule and can be decomposed into components that measure both discriminative performance and calibration.

$$BS(t) = \mathbb{E}_{\mathcal{D}} \left[\left(\mathbb{1}\{T > t\} - \widehat{\mathbb{P}}(T > t|X) \right)^2 \right]$$

Each of the metrics described above are adjusted for censoring by using standard Thompson-Horvitz style Inverse Propensity of Censoring Weights (IPCW) estimates learnt with a Kaplan-Meier estimator over the censoring times. Details are in Appendix B.

2.9 Experimental Protocol

For the proposed model, DCM and the baselines we perform 5-fold cross validation. The predictions of each fold at the 25th, 50th and 75th quantiles of event times are collapsed together and bootstrapped in order to generate standard errors. For the proposed

model and the baselines we report the mean of the evaluation metric and the bootstrapped[‡] standard errors for the model that has the lowest Brier Score amongst all the competing set of hyper parameter choices. For DCM, the set of hyperparameter choices include the number of hidden layers for Φ tuned from $\{1, 2\}$, units in each hidden layer selected from $\{50, 100\}$, the number of mixture components K which are tuned between $\{3, 4, 6\}$ and the discounting factor for the VAE-Loss, α tuned from $\{0, 1\}$. Optimization is performed using the Adam optimizer (Kingma and Ba, 2014) in tensorflow with learning rates fixed 1×10^{-3} and mini batch size of 128. The Baseline Survival Splines are fixed to be of degree 3 and fit using the scipy python package.

3 RESULTS

In this section we describe the results of our various experiments with DCM and the competing baselines. We evaluate discriminative performance and calibration for DCM against the baselines on the three datasets for the entire population as well as the minority demographic in Figures 3 and 4 respectively. (For tabulated results including AuROC and Brier Scores, refer to D.1.)

FLCHAIN: DCM beat all the other baselines in terms of discriminative performance on the entire population as well as on the minority, ‘Female’ subgroup. In terms of calibration DCM was also consistently better than all the other baselines as evidenced from low ECE scores. Interestingly, both the FSN and the linear Cox model did poorly in terms of concordance and calibration while DCM had good performance suggesting it is not sensitive to proportional hazards (PH).

SUPPORT: For the SUPPORT dataset, RSF had the best discriminative performance at a population level, and DCM came a close second beating the other deep learning baselines. Interestingly we found that the proposed DCM had the best discriminative performance on the minority demographic beating all other baselines including RSF. While RSF was strong in terms of discriminative performance, it was also the most poorly calibrated as compared to the other baselines. DCM had the lowest ECE at each quantile amongst all baselines, at both the population level as well as on the minority demographic. The performance of FSN was close to DCM in terms of calibration but did poorly in terms of discrimination, further lending evidence to the fact that DCM is not restricted by PH.

[‡]100 times

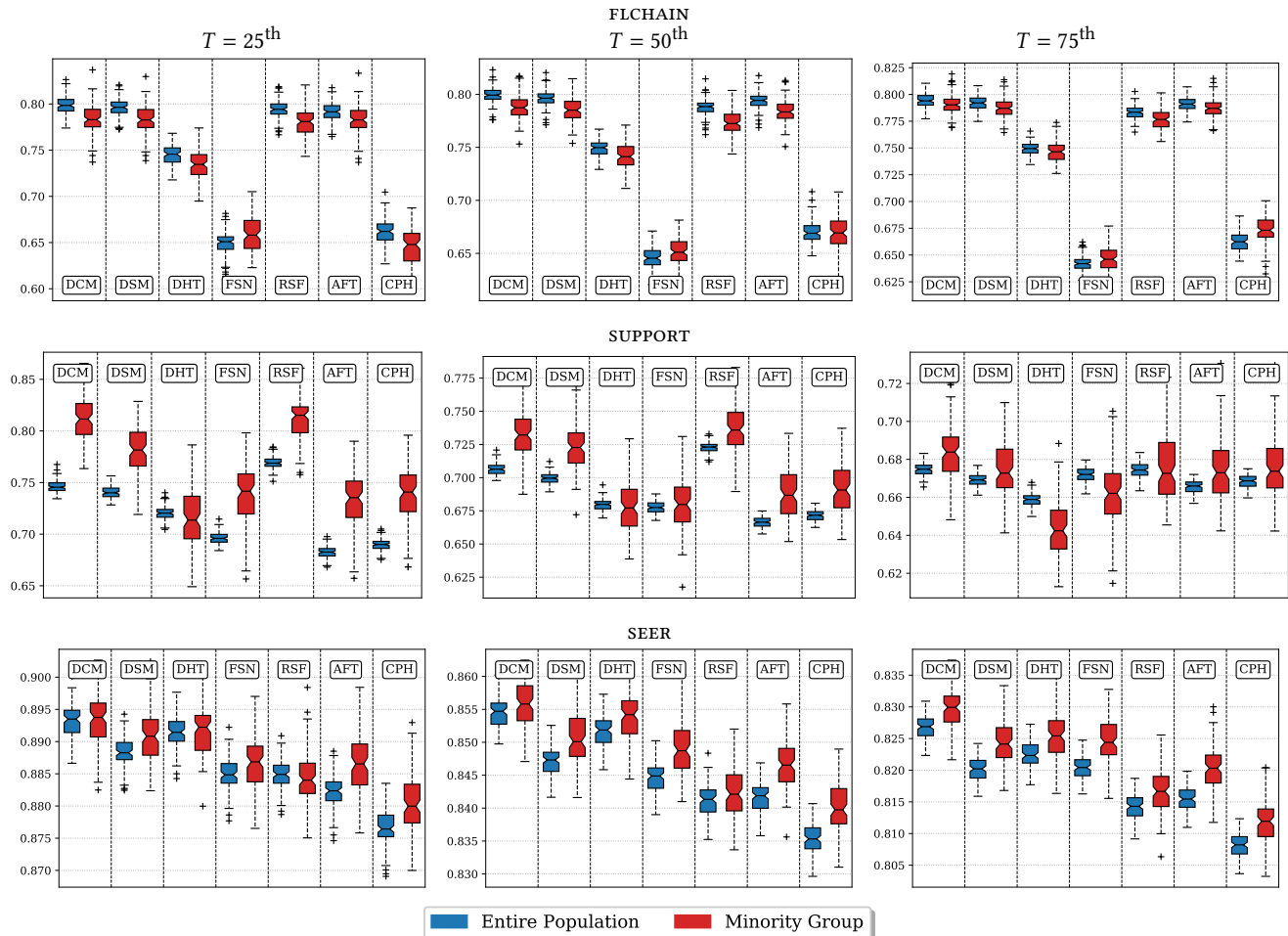


Figure 3: C^{td} (higher means better discrimination) of proposed approach versus baselines at different quantiles of event times. The columns represents different quantiles at which we evaluate the individual metrics.

SEER: In terms of discriminative performance, DCM beat all the other baselines at all quantiles of interest for the entire population as well as for the minority group. DCM also consistently had lower ECE as compared to the other models. We found that DHT was a strong competitor, which is understandable since it is particularly well suited for discrete time datasets like SEER. Note that in the case of SEER we also report results stratified by the four largest minority demographics in the subset of the dataset we work with in Figure 5. DCM has better discriminative performance across groups especially at longer horizons of event times. In terms of calibration, DCM comes close to or outperforms the semi-parametric approaches like FSN/DeepSurv.

In order to assess the influence of the protected attribute to determine the outcome we conduct additional studies involving removal of the protected attribute (unawareness) and training decoupled classifiers for each demographic. We find that in the case of unawareness we ended up with poorer calibration while decoupled classifiers had poor discriminative performance. These results are deferred to Appendices D.2 and D.3.

4 DISCUSSION

Survival prediction and disease prognosis models can help doctors give patients and their caregivers better recommendations and care, we emphasize that the intended uses of survival predictions in medicine is to help healthcare providers understand where to focus their care—particularly for preventive interventions—to have the most potential benefit. Ensuring calibration across demographics is a step towards making models more equitable especially when risk to a particular demographic is systematically being mis-estimated. One example is the 2013 ACC/AHA[§] Pooled Cohort Equations (PCE) to assess cardio-vascular risk (Stone et al., 2014). Yadlowsky et al. demonstrate that 2013 PCEs overestimate the risk for approximately 11.8 million U.S. adults and this overestimation is especially prominent amongst the black population.

However, survival predictions have limitations. For example, studies show that in the US, Black women with breast cancer have a higher mortality rate than White women (Yedjou et al., 2019).

[§]American College of Cardiology/American Heart Association

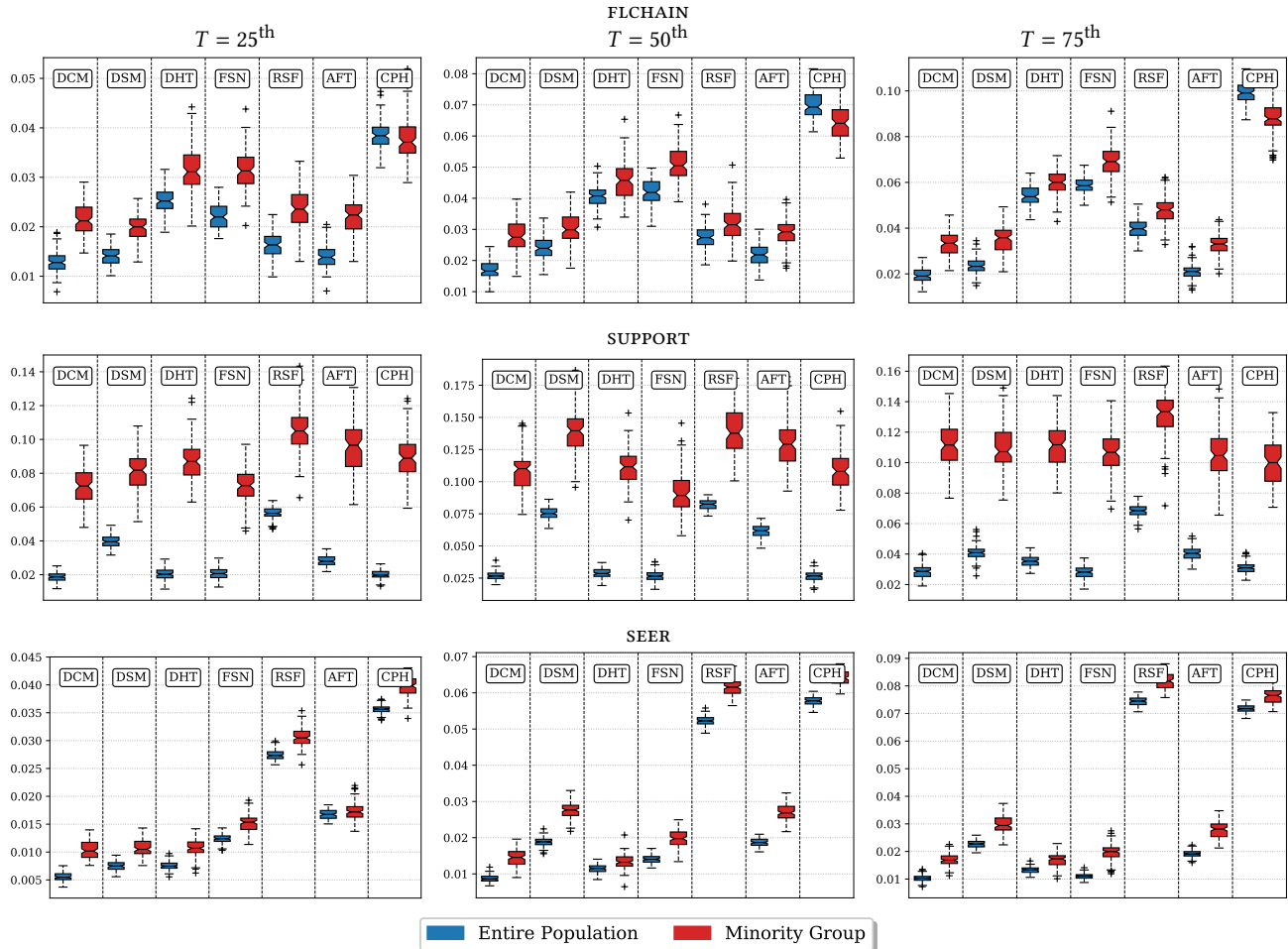


Figure 4: ECE (lower means better calibration) of proposed approach versus baselines at different quantiles of event times. The columns represents different quantiles at which we evaluate the individual metrics.

However, there is an ongoing discussion on whether the mortality rate is related to hereditary characteristics (Yedjou et al., 2019), other factors such as late diagnosis due to historical discrimination, or a combination of all these factors (George et al., 2015). The datasets used in these studies may have unobserved confounding characteristics that may be causally related to the final outcome (Gaïlle et al., 2020). As a result, the extent to which the reported effects of protected attributes like ‘Race’ and ‘Gender’¹ are causal is problem dependent, unclear in the settings studied here, and an open research problem (Dwork et al., 2012) beyond the scope of this paper. Following Mitchell et al. (2019), we believe risk predictions should not be used to make fully automated decisions like assessing insurance policy premiums (Chiang, 1984; Czado and Rudolph, 2002), for immigration status recommendations, or for triage in cases of scarce resources, such as life support systems.

¹Given that ‘Race’, ‘Gender’ are not clearly defined attributes even in medical contexts, we urge readers to exercise caution before including these attributes in a model.

5 RELATED WORK

Recent progress in Deep Learning has also sparked interest in the Survival Analysis community. Recent thrusts in survival analysis have involved Deep Learning based Cox models (Katzman et al., 2018) like the original Faraggi-Simon network (Faraggi and Simon, 1995). More recent papers have explored the use of Discrete time models (Lee et al., 2018), recurrent neural architectures (Lee et al., 2019a) as well as fully parametric methods (Nagpal et al., 2020) for modelling survival outcomes in the presence of censoring. More involved techniques have involved the use of ensembles with black box optimization, auto encoding variational bayes (Chapfuwa et al., 2020; Xiu et al., 2020), as well as adversarial methods (Chapfuwa et al., 2018) to estimate survival outcomes.

Attempts to learn a mixture of Cox models (Nagpal et al., 2019; Rosen and Tanner, 1999) have focused primarily on learning a mixture of log-linear parametric components for the hazard ratio in the partial log-likelihood. These approaches are still subject to the strong assumptions of proportional hazards. Towards the best of our knowledge, our approach is the first attempt at learning a Cox

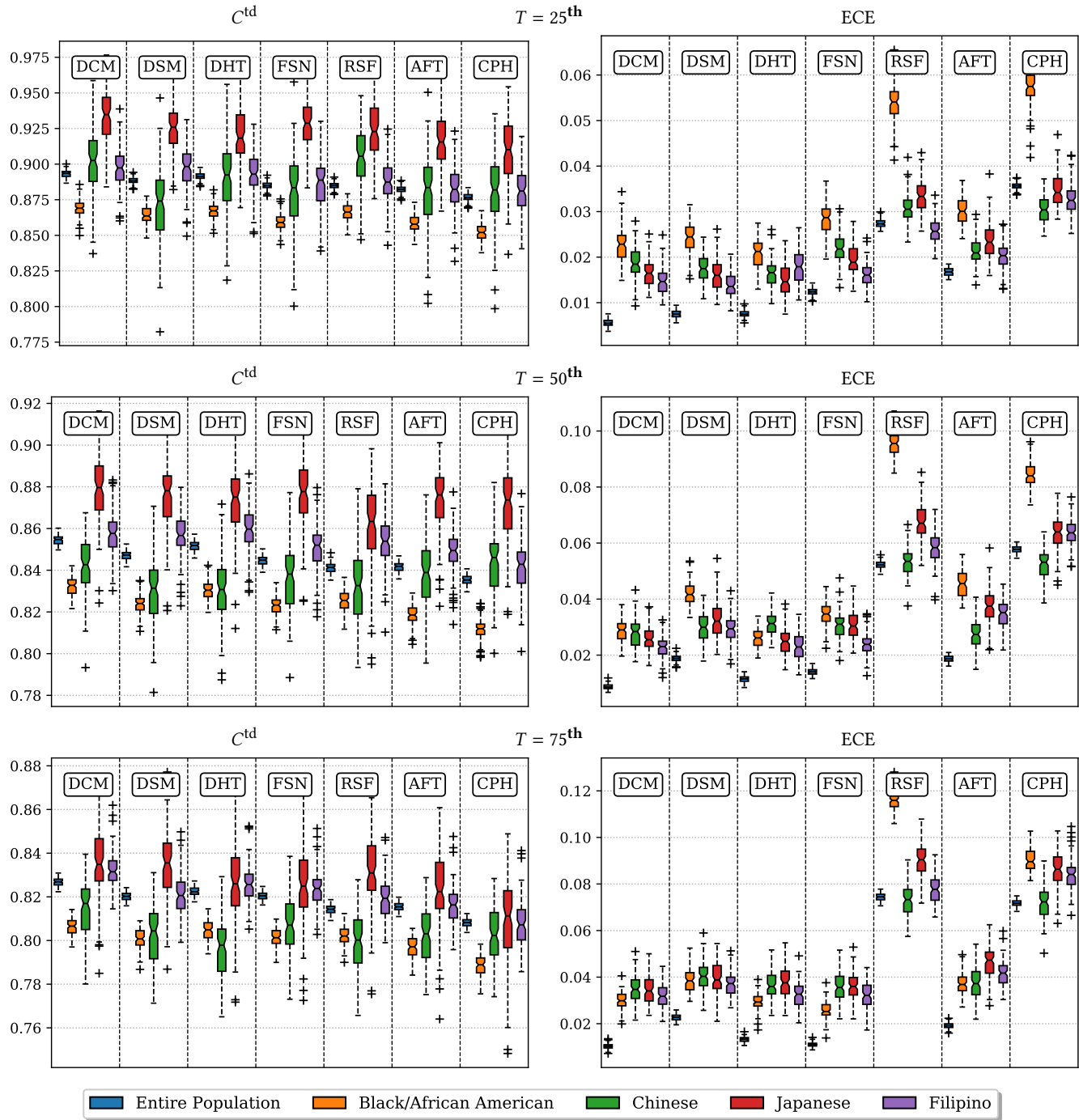


Figure 5: C^{td} (higher means better discrimination) and ECE (lower means better calibration) of proposed approach versus baselines at different quantiles of event times for the minority demographics. The rows represent different quantiles at which we evaluate the individual metrics. (Minorities in the dataset are denoted by different colors in the legend)

mixture model using the full likelihood and jointly estimating both the parametric relative hazard and the baseline hazard functions. Close lines of work to ours include [Chapfuwa et al. \(2020\)](#); [Ranganath et al. \(2016\)](#), where the authors propose the latent space

to be a mixture distribution and sample the outcome event time from a parametric decoder. Our approach differs from this as we do not need to make any strong parametric assumptions on the event outcome times.

There has also been an interest in learning survival models on time-series and temporal data (Lee et al., 2019a). In this paper we restrict our approach to the case with static feature snapshots, although since our approach involves representation learning using neural networks, it can be easily extended to these settings with appropriate choice of recurrent neural networks.

Poor calibration of deep learning methods has been explored recently in machine learning literature (Guo et al., 2017; Nixon et al., 2019). Poor calibration of Deep Learning models in areas like Natural Language Processing (Nguyen and O'Connor, 2015) and Computer Vision has also been demonstrated. Existing lines of research to improve calibration have involved post processing techniques like Platt Scaling, Bayesian and ensemble methods as well as IPM penalties (Kumar et al., 2018) to improve model calibration. Calibration in the specific case of survival models has been an active area of research as well. Lee et al. (2019b) proposed an ensemble of multiple survival analysis models weighted using Black-Box Bayesian optimization for better calibration. This makes for an interesting modelling approach but practical application is challenging due to computational complexity.

Literature in algorithmic fairness has proposed calibration over subgroups as a measure of algorithm fairness (Kleinberg et al., 2016; Chouldechova, 2017; Pleiss et al., 2017). In these works, calibration is typically referred to as ‘sufficiency’ or ‘matching conditional frequencies’ (Hardt et al., 2016) and evaluated using reliability diagrams. We stress that as opposed to scenarios where an algorithm is employed to determine the assignment to a service, in healthcare we are typically interested in estimating risk. In as much errors on both sides (under and over estimation) of the risk are potentially unfair making calibration a well suited metric for fairness evaluation.*

Survival analysis scenarios are also prone to censoring, making estimation of the Expected Calibration Error challenging. Methods involving evaluation for calibration in the presence of censoring have involved simple histogram based binning methods followed by Kaplan-Meier or IPCW estimation of the Survival probability within each bin. More involved recent methods involve non parametric methods like regression splines (Austin et al., 2020) and kernel methods (Yadlowsky et al., 2019). In this tradition, we shine the light on the calibration of models in our empirical evaluations, emphasizing the calibration within minority groups, in particular. We find that without sacrificing discriminative performance, the added flexibility of our mixture model improves calibration, overall and especially in minority groups.

6 CONCLUSION

We proposed ‘Deep Cox Mixtures’ to model censored Time-to-Event data. Our approach involves estimating hazard ratios within latent clusters followed by non-parametric estimation of the baseline survival rates but is not limited by the strong assumptions of constant proportional hazards. We experiment with several real-world health datasets and demonstrate superiority of our approach both in terms of discriminative performance and calibration.

*In healthcare, it is typically ethical to include demographic information like race and gender when estimating outcomes. If there are strong reasons to believe that such information does not cause the outcome, other definitions of algorithmic fairness might be more valid.

REFERENCES

- Austin, P. C., Harrell Jr, F. E., and van Klaveren, D. (2020). Graphical calibration curves and the integrated calibration index (ici) for survival models. *Statistics in Medicine*.
- Breslow, N. E. (1972). Contribution to discussion of paper by dr cox. *J. Roy. Statist. Soc., Ser. B*, 34:216–217.
- Chapfuwa, P., Li, C., Mehta, N., Carin, L., and Henao, R. (2020). Survival cluster analysis. In *Proceedings of the ACM Conference on Health, Inference, and Learning*, pages 60–68.
- Chapfuwa, P., Tao, C., Li, C., Page, C., Goldstein, B., Carin, L., and Henao, R. (2018). Adversarial time-to-event modeling. *arXiv preprint arXiv:1804.03184*.
- Chiang, C. L. (1984). *The life table and its applications*. Krieger Malabar, FL.
- Chouldechova, A. (2017). Fair prediction with disparate impact: A study of bias in recidivism prediction instruments. *Big data*, 5(2):153–163.
- Connors, A. F., Dawson, N. V., Desbiens, N. A., Fulkerson, W. J., Goldman, L., Knaus, W. A., Lynn, J., Oye, R. K., Bergner, M., Damiano, A., et al. (1995). A controlled trial to improve care for seriously ill hospitalized patients: The study to understand prognoses and preferences for outcomes and risks of treatments (support). *Jama*, 274(20):1591–1598.
- Cox, D. R. (1972). Regression models and life-tables. *Journal of the Royal Statistical Society: Series B (Methodological)*, 34(2):187–202.
- Czado, C. and Rudolph, F. (2002). Application of survival analysis methods to long-term care insurance. *Insurance: Mathematics and Economics*, 31(3):395–413.
- Dempster, A. P., Laird, N. M., and Rubin, D. B. (1977). Maximum likelihood from incomplete data via the em algorithm. *Journal of the Royal Statistical Society: Series B (Methodological)*, 39(1):1–22.
- Dispenzieri, A., Katzmann, J. A., Kyle, R. A., Larson, D. R., Therneau, T. M., Colby, C. L., Clark, R. J., Mead, G. P., Kumar, S., Melton III, L. J., et al. (2012). Use of nonclonal serum immunoglobulin free light chains to predict overall survival in the general population. In *Mayo Clinic Proceedings*, volume 87, pages 517–523. Elsevier.
- Dwork, C., Hardt, M., Pitassi, T., Reingold, O., and Zemel, R. (2012). Fairness through awareness. In *Proceedings of the 3rd innovations in theoretical computer science conference*, pages 214–226.
- Faraggi, D. and Simon, R. (1995). A neural network model for survival data. *Statistics in medicine*, 14(1):73–82.
- Gaille, M., Aranedo, M., Dubost, C., Guillermain, C., Kaakai, S., Ricadat, E., Todd, N., and Rera, M. (2020). Ethical and social implications of approaching death prediction in humans-when the biology of ageing meets existential issues. *BMC Medical Ethics*, 21(1):1–13.
- George, P., Chandwani, S., Gabel, M., Ambrosone, C. B., Rhoads, G., Bandera, E. V., and Demissie, K. (2015). Diagnosis and surgical delays in african american and white women with early-stage breast cancer. *Journal of Women’s Health*, 24(3):209–217.
- Guo, C., Pleiss, G., Sun, Y., and Weinberger, K. Q. (2017). On calibration of modern neural networks. *arXiv preprint arXiv:1706.04599*.
- Hardt, M., Price, E., and Srebro, N. (2016). Equality of opportunity in supervised learning. In *Advances in neural information processing systems*, pages 3315–3323.

- Ishwaran, H., Kogalur, U. B., Blackstone, E. H., Lauer, M. S., et al. (2008). Random survival forests. *The annals of applied statistics*, 2(3):841–860.
- Katzman, J. L., Shaham, U., Cloninger, A., Bates, J., Jiang, T., and Kluger, Y. (2018). Deepsurv: personalized treatment recommender system using a cox proportional hazards deep neural network. *BMC medical research methodology*, 18(1):24.
- Kingma, D. P. and Ba, J. (2014). Adam: A method for stochastic optimization. *arXiv preprint arXiv:1412.6980*.
- Kleinberg, J., Mullainathan, S., and Raghavan, M. (2016). Inherent trade-offs in the fair determination of risk scores. *arXiv preprint arXiv:1609.05807*.
- Kumar, A., Sarawagi, S., and Jain, U. (2018). Trainable calibration measures for neural networks from kernel mean embeddings. In *International Conference on Machine Learning*, pages 2805–2814.
- Lee, C., Yoon, J., and Van Der Schaar, M. (2019a). Dynamic-deephit: A deep learning approach for dynamic survival analysis with competing risks based on longitudinal data. *IEEE Transactions on Biomedical Engineering*, 67(1):122–133.
- Lee, C., Zame, W., Alaa, A., and Schaar, M. (2019b). Temporal quilting for survival analysis. In *The 22nd International Conference on Artificial Intelligence and Statistics*, pages 596–605.
- Lee, C., Zame, W. R., Yoon, J., and van der Schaar, M. (2018). Deephit: A deep learning approach to survival analysis with competing risks. In *Thirty-Second AAAI Conference on Artificial Intelligence*.
- Lin, D. (2007). On the breslow estimator. *Lifetime data analysis*, 13(4):471–480.
- Mitchell, M., Wu, S., Zaldivar, A., Barnes, P., Vasserman, L., Hutchinson, B., Spitzer, E., Raji, I. D., and Gebru, T. (2019). Model cards for model reporting. In *Proceedings of the conference on fairness, accountability, and transparency*, pages 220–229.
- Nagpal, C., Li, X., and Dubrawski, A. (2020). Deep survival machines: Fully parametric survival regression and representation learning for censored data with competing risks.
- Nagpal, C., Sangave, R., Chahar, A., Shah, P., Dubrawski, A., and Raj, B. (2019). Nonlinear semi-parametric models for survival analysis. *arXiv preprint arXiv:1905.05865*.
- Nguyen, K. and O’Connor, B. (2015). Posterior calibration and exploratory analysis for natural language processing models. *arXiv preprint arXiv:1508.05154*.
- Nixon, J., Dusenberry, M. W., Zhang, L., Jerfel, G., and Tran, D. (2019). Measuring calibration in deep learning. In *CVPR Workshops*, pages 38–41.
- Pleiss, G., Raghavan, M., Wu, F., Kleinberg, J., and Weinberger, K. Q. (2017). On fairness and calibration. In *Advances in Neural Information Processing Systems*, pages 5680–5689.
- Ranganath, R., Perotte, A., Elhadad, N., and Blei, D. (2016). Deep survival analysis. *arXiv preprint arXiv:1608.02158*.
- Rosen, O. and Tanner, M. (1999). Mixtures of proportional hazards regression models. *Statistics in Medicine*, 18(9):1119–1131.
- Song, Z., Henao, R., Carlson, D., and Carin, L. (2016). Learning sigmoid belief networks via monte carlo expectation maximization. In *Artificial Intelligence and Statistics*, pages 1347–1355.
- Stone, N. J., Robinson, J. G., Lichtenstein, A. H., Merz, C. N. B., Blum, C. B., Eckel, R. H., Goldberg, A. C., Gordon, D., Levy, D., Lloyd-Jones, D. M., et al. (2014). 2013 acc/aha guideline on the treatment of blood cholesterol to reduce atherosclerotic cardiovascular risk in adults: a report of the american college of cardiology/american heart association task force on practice guidelines. *Journal of the American College of Cardiology*, 63(25 Part B):2889–2934.
- Wei, G. C. and Tanner, M. A. (1990). A monte carlo implementation of the em algorithm and the poor man’s data augmentation algorithms. *Journal of the American statistical Association*, 85(411):699–704.
- Xiu, Z., Tao, C., and Henao, R. (2020). Variational learning of individual survival distributions. In *Proceedings of the ACM Conference on Health, Inference, and Learning*, pages 10–18.
- Yadlowsky, S., Basu, S., and Tian, L. (2019). A calibration metric for risk scores with survival data. In *Machine Learning for Healthcare Conference*, pages 424–450.
- Yadlowsky, S., Hayward, R. A., Sussman, J. B., McClelland, R. L., Min, Y.-I., and Basu, S. (2018). Clinical implications of revised pooled cohort equations for estimating atherosclerotic cardiovascular disease risk. *Annals of internal medicine*, 169(1):20–29.
- Yedjou, C. G., Sims, J. N., Miele, L., Noubissi, F., Lowe, L., Fonseca, D. D., Alo, R. A., Payton, M., and Tchounwou, P. B. (2019). Health and racial disparity in breast cancer. In *Breast Cancer Metastasis and Drug Resistance*, pages 31–49. Springer.

Supplementary Materials

A ADDITIONAL DETAILS ON DCM IMPLEMENTATION

A.1 Non Applicability of the Partial Likelihood for the Proposed Model

In this section, we demonstrate that we cannot directly maximize the partial likelihood to learn our model. In the case of the Cox model, the hazard rate for an individual with covariates \mathbf{x}_i at time t , $\lambda(t|\mathbf{x}_i)$ is given as

$$\lambda(t|\mathbf{x}_i) = \lambda_0(t) \exp(f(\boldsymbol{\theta}, \mathbf{x}_i)).$$

Here, $\lambda_0(t)$ is the baseline hazard. Now the partial likelihood $\mathcal{P}\mathcal{L}(\boldsymbol{\theta})$ is defined as

$$\mathcal{P}\mathcal{L}(\boldsymbol{\theta}) = \prod_{i:\delta_i=1} \frac{\lambda(t|\mathbf{x}_i)}{\sum_{j \in \mathcal{R}(t_i)} \lambda(t|\mathbf{x}_j)} = \prod_{i:\delta_i=1} \frac{\cancel{\lambda_0(t)} \exp(f(\boldsymbol{\theta}; \mathbf{x}_i))}{\sum_{j \in \mathcal{R}(t_i)} \cancel{\lambda_0(t)} \exp(f(\boldsymbol{\theta}; \mathbf{x}_j))} \quad (12)$$

$$= \prod_{i:\delta_i=1} \frac{\exp(f(\boldsymbol{\theta}; \mathbf{x}_i))}{\sum_{j \in \mathcal{R}(t_i)} \exp(f(\boldsymbol{\theta}; \mathbf{x}_j))}. \quad (13)$$

Under our model, the hazard rate for an individual with covariates \mathbf{x}_i at time t , $\lambda(t|\mathbf{x}_i)$ is given as

$$\lambda(\cdot|\mathbf{x}_i) = \frac{\mathbb{P}(t|\mathbf{x}_i)}{S(t|\mathbf{x}_i)} = \frac{\sum_k \mathbb{P}(t|\mathbf{x}_i, Z=k) \mathbb{P}(Z=k|\mathbf{x}_i)}{\sum_k S(t|\mathbf{x}_i, Z=k) \mathbb{P}(Z=k|\mathbf{x}_i)}$$

Clearly, we do not have the proportional hazards form for DCM and so cannot directly optimize the Partial Likelihood independent of the baseline hazard rate.

A.2 Spline Estimates

We want to extract the probabilities estimates $\mathbb{P}(T|Z, X)$ in order to compute the posterior $\mathbb{P}(Z|T, X) \propto \mathbb{P}(T|Z, X)$ for the uncensored observations. We only have access to the estimated survival function from the Breslow's estimate, $\widehat{S}(T > t|X = \mathbf{x}_i)$.

$$\begin{aligned} \mathbb{P}(T > t|X = \mathbf{x}_i, Z = k) &= 1 - \mathbb{P}(T \leq t|X = \mathbf{x}_i, Z = k) \\ &= 1 - \text{cdf}(T \leq t|X = \mathbf{x}_i, Z = k) \end{aligned}$$

$$\text{Now, cdf}(T \leq t|X = \mathbf{x}_i, Z = k) = 1 - \mathbb{P}(T > t|X = \mathbf{x}_i, Z = k)$$

$$\frac{\partial}{\partial t} \text{cdf}(T \leq t|X = \mathbf{x}_i, Z = k) = \frac{\partial}{\partial t} \left(1 - \mathbb{P}(T > t|X = \mathbf{x}_i, Z = k) \right) \quad [\text{taking derivative wrt. } t]$$

$$\begin{aligned} \implies \text{pdf}(T = t|X = \mathbf{x}_i, Z = k) &= -\frac{\partial}{\partial t} \mathbb{P}(T > t|X = \mathbf{x}_i, Z = k) \\ &= -\frac{\partial}{\partial t} S_k(t) \exp(f_k(\boldsymbol{\theta}; \mathbf{x}_i)) \end{aligned}$$

Here pdf(\cdot) and cdf(\cdot) are the probability density and the cumulative density functions respectively. Now replacing the baseline survival function $S_k(\cdot)$ with the interpolated spline estimate, $\widetilde{S}_k(\cdot)$ we get the spline estimate of $\mathbb{P}(T = t|Z, X)$ as

$$\begin{aligned} \widehat{\mathbb{P}}(T = t|Z, X) &= -\frac{\partial}{\partial t} \widetilde{S}_k(t) \exp(f_k(\boldsymbol{\theta}; \mathbf{x}_i)) \\ &= -\exp(f_k(\boldsymbol{\theta}; \mathbf{x}_i)) \widetilde{S}_k(t)^{\exp(f_k(\boldsymbol{\theta}; \mathbf{x}_i)) - 1} \frac{\partial}{\partial t} \widetilde{S}_k(t) \\ &= -\exp(f_k(\boldsymbol{\theta}; \mathbf{x}_i)) \frac{\widehat{\mathbb{P}}(T > t|\mathbf{x}_i, Z = k)}{\widetilde{S}_k(t)} \frac{\partial}{\partial t} \widetilde{S}_k(t) \end{aligned}$$

Here, $\frac{\partial}{\partial t} \widetilde{S}_k(t)$ is the derivative of the baseline survival rate interpolated with a polynomial spline.

B CENSORING ADJUSTED EVALUATION METRICS

Area under ROC Curve (AUC): The ROC curve is defined as a plot between the True Positive Rate/Sensitivity (TPR) and the False Positive Rate (FPR) for all thresholds at which a classifier can be deployed. Note that the FPR is equal to 1–Specificity. We employ the technique proposed by [Uno et al. \(2007\)](#); [Hung and Chiang \(2010\)](#) to adjust the Sensitivity using IPCW estimates of the censoring distribution. The Specificity is computed on the uncensored instances.

$$\widehat{\text{Se}}(c, t) = \frac{\sum_{i=1}^n \omega_i \cdot \mathbb{1}\{\pi_i(t) > c, T_i \leq t\}}{\sum_{i=1}^n \omega_i \cdot \mathbb{1}\{T_i < t\}}; \quad \omega_i = \frac{\delta_i}{n \cdot \hat{G}(T_i)}; \quad \widehat{\text{Sp}}(c, t) = \frac{\sum_{i=1}^n \mathbb{1}\{\pi_i(t) \leq c, T_i > t\}}{\sum_{i=1}^n \mathbb{1}\{T_i > t\}}.$$

$\widehat{\text{Se}}(c, t)$ and $\widehat{\text{Sp}}(c, t)$ refer to the estimated sensitivity and specificity at classification threshold c and time horizon t respectively. $\hat{G}(t)$ is a Kaplan-Meier estimator of the censoring distribution and $\pi_i(t)$ is the estimated survival probability, $\widehat{\mathbb{P}}(T > t|X = \mathbf{x}_i)$ by the classifier. This curve is plotted for all thresholds $c \in [0, 1]$ and the area under the curve is used to AUC. For a larger discussion around comparisons of various strategies to compute ROC curves in the presence of censoring refer to [Kamarudin et al. \(2017\)](#).

Time Dependent Concordance Index (C^{td}): Concordance Index estimates ranking ability by exhaustively comparing relative risks across all pairs of individuals in the test set within a fixed horizon of time.

$$C^{\text{td}}(t) = \mathbb{P}(\pi_i(t) \leq \pi_j(t) | \delta_i = 1, T_i < T_j, T_i \leq t)$$

Here, $\pi_i(t)$ is the estimated survival probability; T represent the event times. In order to deal with censoring we employ the censoring adjusted estimator for C^{td} that exploits IPCW estimates from a Kaplan-Meier estimate of the censoring distribution. The details are beyond the scope of this discussion and can be found in [Uno et al. \(2011\)](#) and [Gerds et al. \(2013\)](#).

Expected ℓ_1 Calibration Error (ECE): The ECE measures the average absolute difference between the observed and expected (according to the risk score) event rates, conditional on the estimated risk score. At time t , let the predicted risk score be $R(t) = \widehat{\mathbb{P}}(T > t|X)$. Then, the ECE approximates

$$\text{ECE}(t) = \mathbb{E}[|\mathbb{P}(T > t|R(t)) - R(t)|]$$

by partitioning the risk scores R into q quantiles $\{[r_j, r_{j+1})\}_{j=1}^q$, and computing the Kaplan-Meier estimate of the event rate $\text{KM}_j(t) \approx \mathbb{P}(T > t|R \in [r_j, r_{j+1}))$, and the average risk score $\bar{R}_j = \frac{1}{n} \sum_{i: R_i \in [r_j, r_{j+1})} R_i$ in each bin. Altogether, the estimated ECE is

$$\widehat{\text{ECE}}(t) = \frac{1}{q} \sum_{j=1}^q |\text{KM}_j(t) - \bar{R}_j(t)|.$$

In practice, we fix the number of quantiles to be 20 for our experiments.

Brier Score (BS): The Brier Score involves computing the Mean Squared Error around the binary forecast of survival at a certain event quantile of interest. Brier Score is a proper scoring rule and can be decomposed into components that measure both discriminative performance and calibration.

$$\begin{aligned} \text{BS}(t) &= \mathbb{E}_{\mathcal{O}} [(\mathbb{1}\{T_i > t\} - \widehat{\mathbb{P}}(T > t|X))^2] \\ \widehat{\text{BS}}_{\text{IPCW}}(t) &= \frac{1}{n} \sum_{i=1}^n \left[\frac{\pi_i(t)^2 \mathbb{1}\{T \leq t, \delta_i = 1\}}{\hat{G}_i(T_i)} + \frac{(1 - \pi_i(t))^2 \mathbb{1}\{T > t\}}{\hat{G}_i(t)} \right]; \\ &\text{where, } \pi_i(t) = \widehat{\mathbb{P}}(T > t|X_i) \end{aligned}$$

The adjusted Brier Score adjusted for Censoring using IPCW is given by $\widehat{\text{BS}}_{\text{IPCW}}(t)$ as proposed in ([Graf et al., 1999](#); [Gerds and Schumacher, 2006](#)) Here, $\hat{G}(\cdot)$ is the Kaplan Meier estimate of the Censoring Distribution. When the Censoring distribution is independent of the Event distribution, the above quantity is an unbiased estimate of the Brier Score.

C HYPER-PARAMETER TUNING FOR THE BASELINES

In this section we specify the hyper parameter choices along with a short description over which we perform grid search for the baselines.

Table 2: DSM Hyper-parameter Grid

Hyper-parameter	Grid
Outcome Distribution	{ 'Weibull' }
No. Clusters (k)	{ '3', '4' }
No. of Hidden Layers	{ '0', '1', '2' }
Hidden Layer Dim.	{ '50', '100' }
Batch Size	{ '128', '256' }
Learning Rate	{ '1e-4', '1e-3' }
Activation	{ 'SeLU' }

Deep Survival Machines (DSM): The choice of hyper parameters for DSM include the number of underlying survival distributions (k) the choice of each outcome survival distribution, the number of hidden layers and neurons for the representation learning network and the activations. We also tune the learning rate and batch size. The choices of hyperparam values is given in Table 2.

Table 3: DHT and FSN Hyper-parameter Grid

Hyper-parameter	Grid
No. of Hidden Layers	{ '1', '2' }
Hidden Layer Dim.	{ '50', '100' }
Batch Size	{ '128', '256' }
Learning Rate	{ '1e-4', '1e-3' }
Activation	{ 'ReLU' }

Deep Hit (DHT): For Deep Hit, we tune the the Number of Hidden Layers, dimensionality of the hidden layers and the activation function. We also tune the learning rate and minibatch size. Note that Deep Hit requires grid discretization of the output event time space. For the SUPPORT and FLCHAIN datasets we discretize the output grid by dividing it into bins of $\max(T)$ bins. Since, the SEER is a discrete event time dataset we divide the output grid for Deep Hit into $\max(T)/10$ bins.

Faraggi-Simon Net (FSN)/DeepSurv: Similar to Deep Hit, for FSN we tune the the Number of Hidden Layers, dimensionality of the hidden layers and the activation function. We also tune the learning rate and minibatch size.

Both FSN and DHT were implemented using the `pycox` (Kvamme et al., 2019) python package. Table 3 describes the hyper-parameter choices for both DHT and FSN.

Table 4: RSF Hyper-parameter Grid

Hyper-parameter	Grid
Max Depth	{ '4', '5' }
No. of Trees	{ '10', '25', '50' }

Random Survival Forest (RSF): For the RSF model we tune the number of trees and the maximum depth of each tree using the implementation as part of the `pysurvival` Python package (Fotso et al., 19). Table 4 presents the chosen grid parameters.

Table 5: AFT and CPH Hyper-parameter Grid

Hyper-parameter	Grid
ℓ_2 Penalty	{ '1e-3', '1e-2', '1e-1' }

For **Cox Proportional Hazards (CPH)** and **Accelerated Failure Time (AFT)** the only hyperparameter is the ℓ_2 penalty on the parameters. The grid choice is presented in Table 5

D ADDITIONAL RESULTS

D.1 Tabulated Results

In this section we present tabulated results for our experiments for the entire population and the minority demographic on the three datasets.

$C^{td}(t) (\uparrow)$			
Model	Quantiles		
	$t = 25th$	$t = 50th$	$t = 75th$
CPH	0.66205 ± 0.01426	0.66963 ± 0.01102	0.66214 ± 0.00871
AFT	0.79139 ± 0.01070	0.79384 ± 0.00804	0.79113 ± 0.00595
RSF	0.79406 ± 0.01034	0.78752 ± 0.00799	0.78316 ± 0.00640
FSN	0.64942 ± 0.01270	0.64558 ± 0.00962	0.64216 ± 0.00765
DHT	0.74447 ± 0.01130	0.74860 ± 0.00809	0.74918 ± 0.00621
DSM	0.79624 ± 0.01044	0.79604 ± 0.00791	0.79190 ± 0.00608
DCM	0.79808 ± 0.01037	0.79932 ± 0.00783	0.79436 ± 0.00607

$AUC(t) (\uparrow)$			
Model	Quantiles		
	$t = 25th$	$t = 50th$	$t = 75th$
CPH	0.66796 ± 0.01492	0.68265 ± 0.01197	0.68208 ± 0.00941
AFT	0.80315 ± 0.01104	0.81695 ± 0.00853	0.82573 ± 0.00630
RSF	0.80545 ± 0.01060	0.80909 ± 0.00854	0.81679 ± 0.00701
FSN	0.65603 ± 0.01319	0.65932 ± 0.01045	0.66526 ± 0.00883
DHT	0.75397 ± 0.01162	0.77018 ± 0.00859	0.78000 ± 0.00674
DSM	0.80778 ± 0.01069	0.81868 ± 0.00839	0.82614 ± 0.00654
DCM	0.80986 ± 0.01066	0.82263 ± 0.00830	0.82980 ± 0.00654

$ECE(t) (\downarrow)$			
Model	Quantiles		
	$t = 25th$	$t = 50th$	$t = 75th$
CPH	0.03863 ± 0.00307	0.06993 ± 0.00420	0.09916 ± 0.00443
AFT	0.01413 ± 0.00237	0.02162 ± 0.00335	0.02115 ± 0.00340
RSF	0.01640 ± 0.00244	0.02738 ± 0.00362	0.03992 ± 0.00441
FSN	0.02221 ± 0.00264	0.04201 ± 0.00397	0.05850 ± 0.00350
DHT	0.02530 ± 0.00255	0.04065 ± 0.00360	0.05435 ± 0.00417
DSM	0.01409 ± 0.00207	0.02410 ± 0.00364	0.02343 ± 0.00328
DCM	0.01284 ± 0.00219	0.01714 ± 0.00304	0.01936 ± 0.00343

$BS(t)(\downarrow)$			
Model	Quantiles		
	$t = 25th$	$t = 50th$	$t = 75th$
CPH	0.06707 ± 0.00274	0.12111 ± 0.00347	0.16649 ± 0.00367
AFT	0.05842 ± 0.00226	0.09908 ± 0.00275	0.12436 ± 0.00247
RSF	0.05893 ± 0.00227	0.10101 ± 0.00268	0.12814 ± 0.00243
FSN	0.06670 ± 0.00266	0.12154 ± 0.00320	0.16458 ± 0.00303
DHT	0.06654 ± 0.00257	0.11515 ± 0.00290	0.14794 ± 0.00261
DSM	0.05771 ± 0.00224	0.09839 ± 0.00276	0.12375 ± 0.00257
DCM	0.05803 ± 0.00226	0.09754 ± 0.00281	0.12222 ± 0.00257

Table 6: Results for various performance metrics on FLCHAIN (entire population) along with bootstrapped std errors.

$C^{td}(t) (\uparrow)$			
Model	Quantiles		
	$t = 25th$	$t = 50th$	$t = 75th$
CPH	0.64437 ± 0.01926	0.66916 ± 0.01597	0.67369 ± 0.01239
AFT	0.78220 ± 0.01578	0.78384 ± 0.01123	0.78751 ± 0.00870
RSF	0.78045 ± 0.01501	0.77297 ± 0.01221	0.77713 ± 0.00985
FSN	0.65993 ± 0.01873	0.65171 ± 0.01311	0.64660 ± 0.01177
DHT	0.73349 ± 0.01587	0.74184 ± 0.01172	0.74683 ± 0.00950
DSM	0.78303 ± 0.01559	0.78529 ± 0.01142	0.78773 ± 0.00899
DCM	0.78394 ± 0.01627	0.78823 ± 0.01167	0.79047 ± 0.00916

$AUC(t) (\uparrow)$			
Model	Quantiles		
	$t = 25th$	$t = 50th$	$t = 75th$
CPH	0.64915 ± 0.02022	0.68420 ± 0.01747	0.69830 ± 0.01356
AFT	0.79441 ± 0.01633	0.80693 ± 0.01224	0.82293 ± 0.00945
RSF	0.79238 ± 0.01546	0.79420 ± 0.01344	0.81256 ± 0.01078
FSN	0.66734 ± 0.01956	0.66564 ± 0.01448	0.67168 ± 0.01383
DHT	0.74328 ± 0.01636	0.76369 ± 0.01285	0.77777 ± 0.01071
DSM	0.79480 ± 0.01604	0.80780 ± 0.01242	0.82201 ± 0.00984
DCM	0.79596 ± 0.01680	0.81141 ± 0.01275	0.82650 ± 0.01002

$ECE(t) (\downarrow)$			
Model	Quantiles		
	$t = 25th$	$t = 50th$	$t = 75th$
CPH	0.03784 ± 0.00438	0.06416 ± 0.00561	0.08782 ± 0.00706
AFT	0.02208 ± 0.00351	0.02891 ± 0.00445	0.03288 ± 0.00461
RSF	0.02357 ± 0.00388	0.03183 ± 0.00513	0.04751 ± 0.00586
FSN	0.03151 ± 0.00397	0.05099 ± 0.00569	0.06896 ± 0.00697
DHT	0.03160 ± 0.00461	0.04569 ± 0.00631	0.06024 ± 0.00569
DSM	0.01999 ± 0.00282	0.03007 ± 0.00492	0.03522 ± 0.00564
DCM	0.02140 ± 0.00323	0.02774 ± 0.00486	0.03326 ± 0.00556

$BS(t)(\downarrow)$			
Model	Quantiles		
	$t = 25th$	$t = 50th$	$t = 75th$
CPH	0.06931 ± 0.00433	0.12231 ± 0.00531	0.16263 ± 0.00570
AFT	0.06129 ± 0.00353	0.10310 ± 0.00402	0.12617 ± 0.00366
RSF	0.06126 ± 0.00354	0.10466 ± 0.00413	0.13054 ± 0.00392
FSN	0.06888 ± 0.00406	0.12426 ± 0.00485	0.16603 ± 0.00508
DHT	0.06859 ± 0.00419	0.11782 ± 0.00456	0.14876 ± 0.00428
DSM	0.06047 ± 0.00352	0.10245 ± 0.00407	0.12618 ± 0.00372
DCM	0.06085 ± 0.00350	0.10144 ± 0.00410	0.12420 ± 0.00383

Table 7: Results for various performance metrics on FLCHAIN (minority) along with bootstrapped std errors.

Tables 6 and 7 present the C^{td} , AUC, ECE and Brier Score for the Entire Population and Minority Demographic on the FLCHAIN dataset, respectively.

$C^{td}(t) (\uparrow)$			
Model	Quantiles		
	$t = 25th$	$t = 50th$	$t = 75th$
CPH	0.68988 ± 0.00574	0.67127 ± 0.00398	0.66859 ± 0.00342
AFT	0.68260 ± 0.00572	0.66624 ± 0.00395	0.66570 ± 0.00339
RSF	0.76917 ± 0.00557	0.72273 ± 0.00403	0.67444 ± 0.00380
FSN	0.69568 ± 0.00610	0.67737 ± 0.00439	0.67193 ± 0.00368
DHT	0.72052 ± 0.00667	0.67958 ± 0.00439	0.65869 ± 0.00368
DSM	0.74082 ± 0.00596	0.69947 ± 0.00398	0.66908 ± 0.00340
DCM	0.74608 ± 0.00605	0.70634 ± 0.00417	0.67448 ± 0.00341

$AUC(t) (\uparrow)$			
Model	Quantiles		
	$t = 25th$	$t = 50th$	$t = 75th$
CPH	0.70109 ± 0.00608	0.69904 ± 0.00485	0.72138 ± 0.00492
AFT	0.69360 ± 0.00605	0.69434 ± 0.00485	0.72094 ± 0.00491
RSF	0.78184 ± 0.00616	0.75042 ± 0.00484	0.72966 ± 0.00523
FSN	0.70663 ± 0.00647	0.70620 ± 0.00524	0.72226 ± 0.00498
DHT	0.73046 ± 0.00688	0.70247 ± 0.00516	0.70389 ± 0.00491
DSM	0.75586 ± 0.00639	0.72894 ± 0.00491	0.72371 ± 0.00503
DCM	0.76165 ± 0.00653	0.73442 ± 0.00489	0.72376 ± 0.00487

$ECE(t) (\downarrow)$			
Model	Quantiles		
	$t = 25th$	$t = 50th$	$t = 75th$
CPH	0.02006 ± 0.00288	0.02647 ± 0.00375	0.03097 ± 0.00408
AFT	0.02813 ± 0.00309	0.06169 ± 0.00481	0.04022 ± 0.00458
RSF	0.05657 ± 0.00334	0.08218 ± 0.00390	0.06851 ± 0.00429
FSN	0.02085 ± 0.00329	0.02663 ± 0.00387	0.02781 ± 0.00399
DHT	0.02048 ± 0.00331	0.02865 ± 0.00393	0.03524 ± 0.00361
DSM	0.03961 ± 0.00335	0.07543 ± 0.00455	0.04073 ± 0.00461
DCM	0.01867 ± 0.00254	0.02671 ± 0.00321	0.02822 ± 0.00409

$BS(t) (\downarrow)$			
Model	Quantiles		
	$t = 25th$	$t = 50th$	$t = 75th$
CPH	0.13338 ± 0.00234	0.19946 ± 0.00185	0.21345 ± 0.00158
AFT	0.13537 ± 0.00252	0.20506 ± 0.00230	0.21469 ± 0.00161
RSF	0.12556 ± 0.00227	0.19347 ± 0.00161	0.21548 ± 0.00115
FSN	0.13224 ± 0.00240	0.19731 ± 0.00201	0.21289 ± 0.00176
DHT	0.12822 ± 0.00247	0.19858 ± 0.00187	0.21939 ± 0.00135
DSM	0.12953 ± 0.00250	0.19971 ± 0.00234	0.21396 ± 0.00160
DCM	0.12457 ± 0.00237	0.19017 ± 0.00194	0.21216 ± 0.00170

Table 8: Results for various performance metrics on SUPPORT (entire population) along with bootstrapped std. errors.

$C^{td}(t) (\uparrow)$			
Model	Quantiles		
	$t = 25th$	$t = 50th$	$t = 75th$
CPH	0.73922 ± 0.02674	0.69129 ± 0.01875	0.67491 ± 0.01565
AFT	0.73290 ± 0.02697	0.68708 ± 0.01896	0.67330 ± 0.01570
RSF	0.81161 ± 0.01948	0.73761 ± 0.01778	0.67471 ± 0.01688
FSN	0.73868 ± 0.02933	0.67990 ± 0.01892	0.66280 ± 0.01605
DHT	0.71602 ± 0.02888	0.67763 ± 0.01772	0.64304 ± 0.01558
DSM	0.78214 ± 0.02369	0.72265 ± 0.01710	0.67485 ± 0.01458
DCM	0.81236 ± 0.02091	0.73252 ± 0.01696	0.68376 ± 0.01397

$AUC(t) (\uparrow)$			
Model	Quantiles		
	$t = 25th$	$t = 50th$	$t = 75th$
CPH	0.72869 ± 0.02772	0.72539 ± 0.02181	0.71221 ± 0.02131
AFT	0.72155 ± 0.02817	0.72187 ± 0.02214	0.71282 ± 0.02130
RSF	0.81873 ± 0.02140	0.77010 ± 0.02107	0.71715 ± 0.02491
FSN	0.72483 ± 0.03014	0.70793 ± 0.02133	0.69215 ± 0.02145
DHT	0.70492 ± 0.02900	0.70620 ± 0.02007	0.67684 ± 0.02162
DSM	0.78398 ± 0.02473	0.75749 ± 0.01933	0.71510 ± 0.02139
DCM	0.81624 ± 0.02193	0.76199 ± 0.02079	0.71164 ± 0.01936

$ECE(t) (\downarrow)$			
Model	Quantiles		
	$t = 25th$	$t = 50th$	$t = 75th$
CPH	0.08999 ± 0.01341	0.10842 ± 0.01531	0.10111 ± 0.01608
AFT	0.09608 ± 0.01481	0.12971 ± 0.01904	0.10530 ± 0.01582
RSF	0.10503 ± 0.01308	0.13928 ± 0.01804	0.13112 ± 0.01512
FSN	0.07285 ± 0.01092	0.09207 ± 0.01655	0.10763 ± 0.01382
DHT	0.08696 ± 0.01179	0.11155 ± 0.01421	0.11131 ± 0.01435
DSM	0.08175 ± 0.01237	0.13929 ± 0.01641	0.10855 ± 0.01598
DCM	0.07280 ± 0.01079	0.10774 ± 0.01576	0.11191 ± 0.01415

$BS(t) (\downarrow)$			
Model	Quantiles		
	$t = 25th$	$t = 50th$	$t = 75th$
CPH	0.13107 ± 0.00873	0.19664 ± 0.00803	0.21505 ± 0.00677
AFT	0.13444 ± 0.00943	0.20687 ± 0.00969	0.21733 ± 0.00704
RSF	0.12535 ± 0.00810	0.19752 ± 0.00684	0.21686 ± 0.00493
FSN	0.12816 ± 0.00850	0.20088 ± 0.00805	0.22418 ± 0.00826
DHT	0.13467 ± 0.00832	0.20729 ± 0.00581	0.22826 ± 0.00620
DSM	0.12787 ± 0.00873	0.20315 ± 0.00903	0.21666 ± 0.00621
DCM	0.11684 ± 0.00851	0.18516 ± 0.00882	0.21641 ± 0.00706

Table 9: Results for various performance metrics on SUPPORT (minority) along with bootstrapped std. errors.

Tables 8 and 9 present the C^{td} , AUC, ECE and Brier Score for the Entire Population and Minority Demographic on the SUPPORT dataset, respectively.

$C^{td}(t) (\uparrow)$			
Model	Quantiles		
	$t = 25th$	$t = 50th$	$t = 75th$
CPH	0.87659 ± 0.00272	0.83536 ± 0.00241	0.80824 ± 0.00202
AFT	0.88226 ± 0.00258	0.84159 ± 0.00241	0.81547 ± 0.00196
RSF	0.88488 ± 0.00233	0.84119 ± 0.00235	0.81418 ± 0.00201
FSN	0.88495 ± 0.00248	0.84474 ± 0.00234	0.82035 ± 0.00191
DHT	0.89147 ± 0.00240	0.85168 ± 0.00236	0.82244 ± 0.00204
DSM	0.88825 ± 0.00224	0.84707 ± 0.00229	0.82016 ± 0.00192
DCM	0.89326 ± 0.00241	0.85450 ± 0.00220	0.82681 ± 0.00189

$AUC(t) (\uparrow)$			
Model	Quantiles		
	$t = 25th$	$t = 50th$	$t = 75th$
CPH	0.88275 ± 0.00278	0.85259 ± 0.00250	0.83369 ± 0.00220
AFT	0.88932 ± 0.00263	0.85958 ± 0.00248	0.84237 ± 0.00210
RSF	0.89065 ± 0.00231	0.85798 ± 0.00245	0.83871 ± 0.00220
FSN	0.89211 ± 0.00257	0.86320 ± 0.00240	0.84773 ± 0.00206
DHT	0.89826 ± 0.00251	0.87014 ± 0.00246	0.84951 ± 0.00218
DSM	0.89526 ± 0.00229	0.86533 ± 0.00240	0.84741 ± 0.00207
DCM	0.90017 ± 0.00248	0.87350 ± 0.00226	0.85519 ± 0.00201

$ECE(t) (\downarrow)$			
Model	Quantiles		
	$t = 25th$	$t = 50th$	$t = 75th$
CPH	0.03562 ± 0.00079	0.05774 ± 0.00120	0.07178 ± 0.00145
AFT	0.01676 ± 0.00084	0.01870 ± 0.00112	0.01917 ± 0.00114
RSF	0.02738 ± 0.00084	0.05234 ± 0.00127	0.07442 ± 0.00162
FSN	0.01239 ± 0.00080	0.01400 ± 0.00108	0.01110 ± 0.00105
DHT	0.00755 ± 0.00075	0.01150 ± 0.00113	0.01327 ± 0.00118
DSM	0.00750 ± 0.00082	0.01881 ± 0.00113	0.02268 ± 0.00135
DCM	0.00552 ± 0.00080	0.00866 ± 0.00096	0.01027 ± 0.00113

$BS(t) (\downarrow)$			
Model	Quantiles		
	$t = 25th$	$t = 50th$	$t = 75th$
CPH	0.05014 ± 0.00067	0.08873 ± 0.00085	0.12057 ± 0.00090
AFT	0.04701 ± 0.00060	0.08266 ± 0.00085	0.11073 ± 0.00091
RSF	0.04795 ± 0.00060	0.08701 ± 0.00080	0.12048 ± 0.00086
FSN	0.04617 ± 0.00060	0.08003 ± 0.00081	0.10747 ± 0.00092
DHT	0.04500 ± 0.00057	0.07880 ± 0.00081	0.10738 ± 0.00096
DSM	0.04581 ± 0.00058	0.08110 ± 0.00084	0.10944 ± 0.00093
DCM	0.04503 ± 0.00058	0.07854 ± 0.00080	0.10641 ± 0.00095

Table 10: Results for various performance metrics on SEER (entire population) along with bootstrapped standard errors.

$C^{td}(t) (\uparrow)$			
Model	Quantiles		
	$t = 25th$	$t = 50th$	$t = 75th$
CPH	0.88037 ± 0.00433	0.84045 ± 0.00388	0.81211 ± 0.00370
AFT	0.88646 ± 0.00423	0.84658 ± 0.00361	0.82038 ± 0.00349
RSF	0.88436 ± 0.00402	0.84217 ± 0.00377	0.81665 ± 0.00336
FSN	0.88699 ± 0.00430	0.84901 ± 0.00375	0.82479 ± 0.00358
DHT	0.89200 ± 0.00393	0.85400 ± 0.00377	0.82548 ± 0.00365
DSM	0.89079 ± 0.00384	0.85062 ± 0.00377	0.82432 ± 0.00360
DCM	0.89333 ± 0.00372	0.85584 ± 0.00355	0.82963 ± 0.00336

$AUC(t) (\uparrow)$			
Model	Quantiles		
	$t = 25th$	$t = 50th$	$t = 75th$
CPH	0.88883 ± 0.00433	0.86044 ± 0.00422	0.83979 ± 0.00418
AFT	0.89515 ± 0.00420	0.86758 ± 0.00386	0.84910 ± 0.00400
RSF	0.89152 ± 0.00403	0.86201 ± 0.00410	0.84357 ± 0.00376
FSN	0.89631 ± 0.00431	0.87022 ± 0.00402	0.85378 ± 0.00407
DHT	0.90016 ± 0.00390	0.87537 ± 0.00412	0.85400 ± 0.00414
DSM	0.89947 ± 0.00385	0.87195 ± 0.00406	0.85349 ± 0.00410
DCM	0.90196 ± 0.00370	0.87745 ± 0.00382	0.85949 ± 0.00380

$ECE(t) (\downarrow)$			
Model	Quantiles		
	$t = 25th$	$t = 50th$	$t = 75th$
CPH	0.03988 ± 0.00178	0.06418 ± 0.00214	0.07635 ± 0.00281
AFT	0.01731 ± 0.00161	0.02710 ± 0.00218	0.02784 ± 0.00286
RSF	0.03065 ± 0.00174	0.06146 ± 0.00233	0.08183 ± 0.00281
FSN	0.01516 ± 0.00161	0.01982 ± 0.00249	0.01963 ± 0.00294
DHT	0.01073 ± 0.00148	0.01340 ± 0.00195	0.01698 ± 0.00243
DSM	0.01083 ± 0.00159	0.02763 ± 0.00222	0.02970 ± 0.00308
DCM	0.01045 ± 0.00162	0.01452 ± 0.00237	0.01692 ± 0.00235

$BS(t) (\downarrow)$			
Model	Quantiles		
	$t = 25th$	$t = 50th$	$t = 75th$
CPH	0.05632 ± 0.00141	0.09890 ± 0.00191	0.12850 ± 0.00202
AFT	0.05217 ± 0.00125	0.09069 ± 0.00186	0.11677 ± 0.00205
RSF	0.05436 ± 0.00136	0.09790 ± 0.00183	0.13000 ± 0.00192
FSN	0.05154 ± 0.00127	0.08767 ± 0.00171	0.11327 ± 0.00201
DHT	0.05091 ± 0.00120	0.08606 ± 0.00172	0.11354 ± 0.00206
DSM	0.05103 ± 0.00118	0.08917 ± 0.00184	0.11559 ± 0.00210
DCM	0.05083 ± 0.00124	0.08622 ± 0.00170	0.11266 ± 0.00199

Table 11: Results for various performance metrics on SEER (minority) along with bootstrapped standard errors.

Tables 10 and 11 and present the C^{td} , AUC, ECE and Brier Score for the Entire Population and Minority Demographic on the SEER dataset, respectively.

D.2 Unawareness to Group Membership

FLCHAIN BS(t) (↓)			
Model	Quantiles		
	$t = 25\text{th}$	$t = 50\text{th}$	$t = 75\text{th}$
AFT	0.05847 ± 0.00225	0.09935 ± 0.00273	0.12486 ± 0.00248
CPH	0.07009 ± 0.00266	0.12779 ± 0.00303	0.17540 ± 0.00278
FSN	0.06604 ± 0.00250	0.11902 ± 0.00280	0.15870 ± 0.00251
DCM	0.05803 ± 0.00226	0.09754 ± 0.00281	0.12222 ± 0.00257

SUPPORT BS(t) (↓)			
Model	Quantiles		
	$t = 25\text{th}$	$t = 50\text{th}$	$t = 75\text{th}$
AFT	0.13538 ± 0.00252	0.20508 ± 0.00235	0.21490 ± 0.00165
CPH	0.13345 ± 0.00236	0.19951 ± 0.00192	0.21363 ± 0.00161
FSN	0.13206 ± 0.00244	0.19777 ± 0.00201	0.21309 ± 0.00188
DCM	0.11684 ± 0.00851	0.18516 ± 0.00882	0.21641 ± 0.00706

SEER BS(t) (↓)			
Model	Quantiles		
	$t = 25\text{th}$	$t = 50\text{th}$	$t = 75\text{th}$
AFT	0.04728 ± 0.00061	0.08327 ± 0.00085	0.11150 ± 0.00092
CPH	0.05031 ± 0.00068	0.08912 ± 0.00085	0.12113 ± 0.00090
FSN	0.04634 ± 0.00060	0.08038 ± 0.00080	0.10797 ± 0.00095
DCM	0.04503 ± 0.00058	0.07854 ± 0.00080	0.10641 ± 0.00095

Table 12: Brier Scores (Lower is better) for various performance metrics along with bootstrapped standard errors on the three datasets compared with baselines unaware of the protected group membership

In the case of CPH and FSN the baseline survival rate is estimated non-parametrically. In Table 12 we attempt to see how unawareness to the demographic compares to Deep Cox Mixtures. Note that we report Brier Score here as it gives sense of both discrimination and calibration.

D.3 Decoupled Survival Models

FLCHAIN BS(t) (↓)			
Model	Quantiles		
	$t = 25\text{th}$	$t = 50\text{th}$	$t = 75\text{th}$
AFT	0.05847 ± 0.00225	0.09935 ± 0.00273	0.12486 ± 0.00248
CPH	0.07009 ± 0.00266	0.12779 ± 0.00303	0.17540 ± 0.00278
FSN	0.06604 ± 0.00250	0.11902 ± 0.00280	0.15870 ± 0.00251
DCM	0.05803 ± 0.00226	0.09754 ± 0.00281	0.12222 ± 0.00257

SUPPORT BS(t) (↓)			
Model	Quantiles		
	$t = 25\text{th}$	$t = 50\text{th}$	$t = 75\text{th}$
AFT	0.13538 ± 0.00252	0.20508 ± 0.00235	0.21490 ± 0.00165
CPH	0.13345 ± 0.00236	0.19951 ± 0.00192	0.21363 ± 0.00161
FSN	0.13206 ± 0.00244	0.19777 ± 0.00201	0.21309 ± 0.00188
DCM	0.11684 ± 0.00851	0.18516 ± 0.00882	0.21641 ± 0.00706

SEER BS(t) (↓)			
Model	Quantiles		
	$t = 25\text{th}$	$t = 50\text{th}$	$t = 75\text{th}$
AFT	0.04728 ± 0.00061	0.08327 ± 0.00085	0.11150 ± 0.00092
CPH	0.05031 ± 0.00068	0.08912 ± 0.00085	0.12113 ± 0.00090
FSN	0.04634 ± 0.00060	0.08038 ± 0.00080	0.10797 ± 0.00095
DCM	0.04503 ± 0.00058	0.07854 ± 0.00080	0.10641 ± 0.00095

Table 13: Brier Scores (Lower is better) for various performance metrics along with bootstrapped standard errors on the three datasets compared with baselines unaware of the protected group membership

In the case of CPH and FSN the baseline survival rate is estimated non-parametrically. In Table 13 we attempt to see how training separate models for each demographic compares to Deep Cox Mixtures by reporting Brier Scores. (Note that we report Brier Score here as it gives sense of both discrimination and calibration.)

SUPPLEMENTARY REFERENCES

- Fotso, S. et al. (2019–). PySurvival: Open source package for survival analysis modeling.
- Gerds, T. A., Kattan, M. W., Schumacher, M., and Yu, C. (2013). Estimating a time-dependent concordance index for survival prediction models with covariate dependent censoring. *Statistics in Medicine*, 32(13):2173–2184.
- Gerds, T. A. and Schumacher, M. (2006). Consistent estimation of the expected brier score in general survival models with right-censored event times. *Biometrical Journal*, 48(6):1029–1040.
- Graf, E., Schmoor, C., Sauerbrei, W., and Schumacher, M. (1999). Assessment and comparison of prognostic classification schemes for survival data. *Statistics in medicine*, 18(17-18):2529–2545.
- Hung, H. and Chiang, C.-t. (2010). Optimal composite markers for time-dependent receiver operating characteristic curves with censored survival data. *Scandinavian journal of statistics*, 37(4):664–679.
- Kamarudin, A. N., Cox, T., and Kolamunnage-Dona, R. (2017). Time-dependent roc curve analysis in medical research: current methods and applications. *BMC medical research methodology*, 17(1):53.
- Kingma, D. P. and Welling, M. (2013). Auto-encoding variational bayes. *arXiv preprint arXiv:1312.6114*.
- Kvamme, H., Borgan, Ø., and Scheel, I. (2019). Time-to-event prediction with neural networks and cox regression. *Journal of machine learning research*, 20(129):1–30.
- Uno, H., Cai, T., Pencina, M. J., D’Agostino, R. B., and Wei, L. (2011). On the c-statistics for evaluating overall adequacy of risk prediction procedures with censored survival data. *Statistics in medicine*, 30(10):1105–1117.
- Uno, H., Cai, T., Tian, L., and Wei, L.-J. (2007). Evaluating prediction rules for t-year survivors with censored regression models. *Journal of the American Statistical Association*, 102(478):527–537.